

An all-glass microfluidic cell for the ABEL trap: fabrication and modeling

Adam E. Cohen

Department of Physics, 382 via Pueblo Mall, Stanford University, Stanford, CA 94305
Department of Chemistry, Stanford University
aecohen@stanford.edu

W. E. Moerner

Department of Chemistry, M/C 5080, 375 North-South Mall, Stanford University, Stanford, CA
94305-5080

ABSTRACT

The Anti-Brownian Electrophoretic trap (ABEL trap) allows a user to trap and manipulate individual fluorescent molecules in solution. The heart of the ABEL trap is a microfluidic cell. In previous incarnations of the ABEL trap, the microfluidic cell was formed from a polydimethylsiloxane (PDMS) stamp and a glass coverslip. Here we present an improved microfluidic cell, made entirely out of glass. This new design significantly decreases the rate of photobleaching, which previously limited the time that a single molecule could be trapped. Chemical modifications to the surface of the cell prevent adsorption and allow one to control the balance between electroosmotic and electrophoretic forces. The depth of the trapping region in the cell can be adjusted to allow trapping of different-sized objects.

Keywords: ABEL trap, single molecule spectroscopy, microfluidics, electrophoresis

Introduction

An ultimate goal of nanotechnology and also of single-molecule research is to trap and manipulate individual molecules in solution. There are many reasons why one might want to trap a single nanoscale object: to study its motion along internal degrees of freedom; to probe its affinity for other molecules that are either free-floating or bound to a surface; to assemble nanomachines one nanoparticle at a time; or to use a fluorescent particle as a light source for imaging other nanoscale structures in its vicinity. All of these applications require precise control and extended observation of a single nanoscale object in solution—a task that requires overcoming the thermal fluctuations in position.

The Anti-Brownian Electrophoretic trap (ABEL trap) enables all of the above applications. We have previously described the hardware and software of the ABEL trap in detail.^{1,2,3} In brief, the ABEL trap tracks the Brownian motion of a single particle of interest by fluorescence microscopy, and then applies a real-time feedback voltage to the solution so that the resulting electrophoretic drift exactly cancels the Brownian motion over some finite temporal bandwidth.

The heart of the ABEL trap is a microfluidic cell. In the center of the cell, a disc-shaped trapping region confines the fluid and molecules to be trapped to a corral tens of microns wide but less than a micron deep. Four microfluidic channels (~80 μm deep, ~1 mm wide, ~7 mm long) radiate outwards from the corners of the trapping region, and terminate in macroscopic electrodes. Applying a voltage $\mathbf{V} = (V_x, V_y)$ to these four electrodes in pairs leads to an electric field and a combined electrophoretic/electroosmotic drift in the trapping region, so that the velocity vector of a particle is $\mathbf{v} \propto \mathbf{V}$.

The microfluidic cell is mounted in a fluorescence microscope. A high-speed, high-sensitivity camera captures up to 300 images/sec of the trapping region. These images are sent to a computer, where custom software extracts in real-time the x,y-coordinates of a single particle of interest. The computer uses this position information to generate a feedback voltage which is applied to the cell. The feedback voltage keeps the particle centered at a target position. The location of the target position can be moved either by specifying a series of coordinates in software, or by clicking and dragging with the computer mouse.

This article describes in detail the fabrication of an all-glass microfluidic cell and a cell-holder for the ABEL trap. The cell and holder are shown in Fig. 1. We present finite-element simulations and analytical calculations to characterize the electrical and mechanical properties of the device.

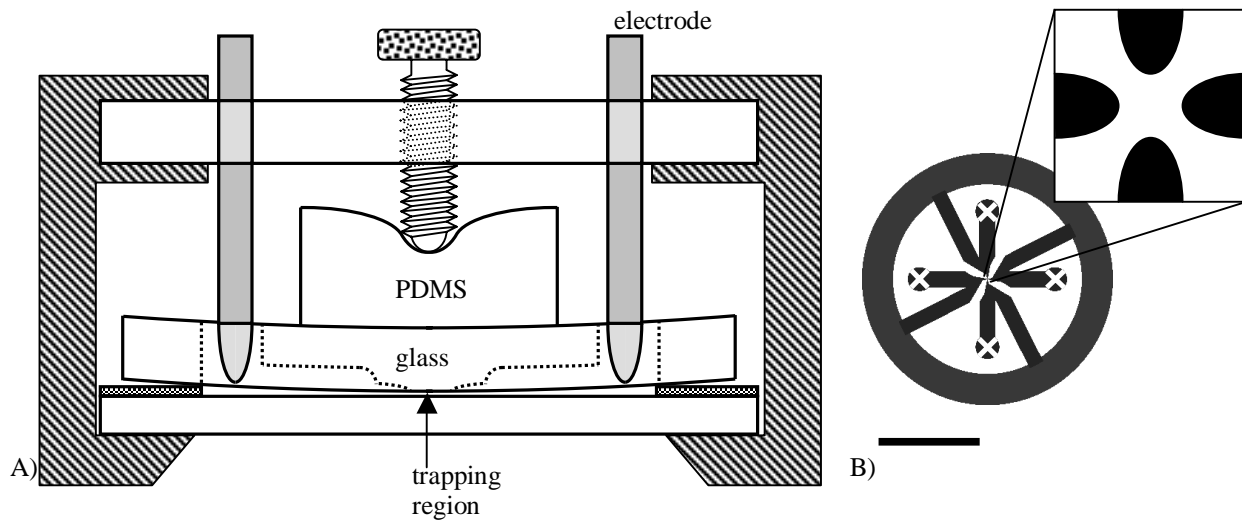


Figure 1: Microfluidic cell for the ABEL trap. A) cross-sectional view. The top of the cell is a patterned glass wafer and the bottom is a standard glass coverslip. A 10 μm annular spacer separates the top and bottom. A setscrew pushes down on a piece of PDMS, which in turn presses on the top piece of glass. The glass bows downward slightly, allowing the depth of the trapping region to be adjusted between 0 – 1 μm . The top and bottom of the cell can be separated for cleaning or surface treatments. B) Top view of the microfluidic channels. Recessed areas are in black. Electrode ports are indicated by white x's. The large circular channel equalizes the hydrostatic pressure in the four arms of the device and allows for easy filling of the channels. The trapping region is in the center. Scale bar, 1 cm. Inset: close-up of the trapping region. The gap between opposing channels is $\sim 130 \mu\text{m}$.

Comparison of glass and PDMS microfluidic cells

The surface chemistry of the microfluidic cell plays a critical role in determining the performance of the ABEL trap. The two most important parameters are adsorption of particles from solution, and the amount of electroosmotic flow (EOF). The frequency with which a particle in the trapping region collides with the walls of the trap is $f_c \approx 2D/d^2$, where D is the diffusion coefficient of the particle and d is the depth of the trapping region. The depth of the trapping region is typically between 100 nm and 1 μm ; much smaller than in most microfluidic devices. Thus the rate of collisions is higher, and so is the probability that a given particle will adsorb to the surface. For a typical scenario with $d = 200 \text{ nm}$ and $D = 20 \mu\text{m}^2/\text{s}$, a particle collides with the walls of the trap roughly 1000 times per second. Adsorbed particles change the surface chemistry of the trap and contribute to an increased fluorescence background. In the very dilute solutions typically used for trapping, adsorption may completely deplete the solution of fluorescent particles. For all of the above reasons, it is important to minimize the affinity of particles for the walls of the trap.

The velocity of a particle in the ABEL trap is given by a combination of the electrophoretic and electroosmotic velocities, $v = v_{eph} + v_{eo}$. The formula for the electrophoretic component, v_{eph} , depends on the ratio of the radius of the particle, a , to the thickness of the Debye layer, h_D . When $a \gg h_D$, v_{eph} is independent of the size of the particle and is given by the Smoluchowski equation: $v_{eph} = E \frac{\zeta_p \epsilon}{\eta}$, where E is the applied field strength, ζ_p is the zeta-potential of the particle, and ϵ and η are the dielectric constant and viscosity, respectively, of the medium surrounding the particle. In the opposite limit of $a \ll h_D$, $v_{eph} = E \frac{q}{6\pi\eta a}$, where, q is the charge on the particle. The electroosmotic velocity is given by $v_{eo} = E \frac{\zeta_w \epsilon}{\eta}$, where ζ_w is the zeta-potential of the wall of the channel. For highly charged analytes, one generally wants to minimize v_{eo} so that the measured mobility reflects intrinsic properties of the particle (i.e. its charge and radius, or its zeta-potential which depends on both charge and geometry). On the other hand, for neutral analytes, electroosmosis provides the only “handle” for applying the feedback, and thus it is necessary to have a strong electroosmotic flow.

A wide variety of surface modifications have been studied for controlling adsorption and electroosmosis in both PDMS and glass capillaries.^{4,5,6,7} Neutral polymer adsorbates can drastically increase the local viscosity within the Debye layer near a channel wall, and thereby decrease the electroosmotic flow. Charged adsorbates, however, may increase the charge density, leading to an increased electroosmotic flow. Hydroxymethylcellulose, hydroxypropylcellulose, and poly(vinyl alcohol) have all been used to decrease adsorption and EOF in glass and silica capillaries. Adsorption and EOF in PDMS channels are best controlled by surface oxidation. The surface of PDMS is naturally highly hydrophobic. It thus strongly adsorbs hydrophobic species from solution, and does not support EOF. Brief exposure to a plasma of room-air or to a corona discharge renders the surface hydrophilic. The modified surface supports EOF, but reverts to hydrophobic over less than an hour if exposed to room-air. For the glass cells that we built, we added to the trapping solution a 10% solution of the polymer POP-6 without the denaturant (a generous gift from Willy Wiyatno at Applied Biosystems).

In the previous incarnation of the ABEL trap², the trapping region was formed by a polydimethylsiloxane (PDMS) stamp and a glass coverslip. This approach had the advantage that the PDMS stamps were easy to make in large numbers and could be disposed after use. For certain applications a PDMS-based trap may be sufficient. We switched to an all-glass trap for four reasons:

- 1) *Better control of surface chemistry* In the PDMS-based trap, one surface in the trapping region was PDMS while the other surface was glass. In general these two surfaces had different electroosmotic velocities. Thus the velocity of a particle in the trap depended on its (uncontrolled) z-displacement. The PDMS and glass also had different affinities for different objects. It was difficult to find a set of solution conditions that were optimal with respect to both surfaces. Furthermore, the surface chemistry of PDMS is poorly defined. PDMS strongly adsorbs species from air and from solution, so its properties change over time.
- 2) *Ability to remove oxygen from the solution* Many fluorophores are quenched by oxygen dissolved in the solution. In most single-molecule experiments, an enzymatic oxygen scavenger system is added, which may extend the lifetime-to-photobleaching of a single molecule by a factor of 10 – 100. PDMS is porous to oxygen, and due to the high surface-to-volume ratio in the trapping region, all attempts at removing oxygen from the solution were unsuccessful. With a glass cell it is much easier to remove the oxygen from the solution. This factor was crucial to trapping single biomolecules for long times.
- 3) *Control of gap thickness* For studies of surface interactions and the effect of electroosmotic flow it is helpful to be able to control the thickness of the trapping region. Below we describe a method for adjusting the thickness of the gap with the glass cells.

- 4) *Lower background fluorescence* PDMS itself has a low level of background fluorescence. Over time, however, it soaks up fluorescent impurities from the environment and the background fluorescence increases. In contrast, glass cells show very low fluorescence and do not absorb impurities.

Fabrication of glass cells

All microfabrication was performed in the Stanford Nanofabrication Facility. The processing steps are outlined in Fig. 2. Transparency masks were designed in Adobe Illustrator and printed at a resolution of 3600 dpi on a mylar transparency. Circular wafers of Corning 7740 glass (700 μm x 100 mm) were cleaned in a Piranha solution (80% Conc. H_2SO_4 , 20% H_2O_2) and then coated with 100 nm of silicon via chemical vapor deposition (CVD). The front side of the wafer was coated with 1.6 μm of Shipley SPR 3612 resist using a standard HMDS prime followed by a spin-coat and soft-bake. The pattern was exposed in a Karl Suss mask aligner (365 nm, 15 mW/cm^2 , 2.5 sec), and developed in Shipley LDD-26 W for 60 s.

The back side of the wafer was then coated with a protection layer of 1.6 μm of SPR 3612 resist. The wafer was given a hard-bake of 115 C for 5 minutes. The front of the wafer was exposed to a reactive-ion etch (RIE) descum (O_2 , 150 mT, 100 sccm, 65 W RF power) immediately followed by a Si etch (SF_6 100 sccm, Freon 22 70 sccm, 100 mT, 55 W) until the exposed Si had been completely removed.

The wafer was then immersed in 49% HF for three minutes (etch rate = 7 $\mu\text{m}/\text{minute}$), with the Si and photoresist acting as a double-layer etch mask (without the photoresist, the HF attacked the glass at pinhole defects in the Si; but the photoresist was incapable of acting as an etch-mask alone). The wafer was thoroughly rinsed in clean water and dried. The resist was stripped from the wafer and the front of the wafer was coated with 18 μm of SPR 220-7 resist. The resist was exposed and developed, leaving a 120 μm circle of resist protecting the trapping region and the channels in the immediate vicinity. The back of the wafer was also coated with 18 μm of SPR 220-7 and the wafer was hard-baked. The wafer was again etched in 49% HF, for 10 minutes. The final depth of the channels was ~ 80 μm , except near the trapping region where they were only 24 μm deep. The channels were not etched to the full depth near the trapping region because the HF etch is isotropic: it widens the channels as it deepens them. Had the channels near the trapping region not been protected, the channels would have fused together.

The wafer was thoroughly rinsed in clean water and the resist was stripped from both faces. Both sides of the wafer were exposed to another RIE polymer descum followed by Si etch, until all of the Si was removed from the wafer. The front of the now-transparent wafer was coated with a protection layer of 7 μm of SPR 220-7, and 0.7 mm holes were drilled in the electrode ports. The wafer was diced into individual cells (9 per wafer; each 25 mm x 25 mm) using a diamond-blade dicing saw, and the protection layer of resist was removed with acetone. The finished chip was cleaned by heating and sonicating in Alconox detergent for 1 hr., followed by a 10 min. etch in an Ar plasma (Harrick).

The bottom piece of glass in the trap was a standard #1 coverslip, 25 mm x 25 mm. The coverslip was cleaned by heating and sonicating in Alconox detergent for 1 hr. A ~ 10 μm tall annular spacer was formed on the coverslip by placing a clean United States nickel over the center of the coverslip and then applying a light coat of spraypaint, with the coin acting as a shadow-mask. The procedure for preparing the coverslip was sufficiently simple that a new coverslip was prepared for each experiment.

Sample holder

A slide holder was machined out of aluminum. A 0-80 setscrew for adjusting the gap was mounted in a sheet of acrylic above the cell. The setscrew pressed on a piece of PDMS, which in turn pressed on the patterned glass. The PDMS acted as a distance divider, turning relatively large displacements of the setscrew into nanometer-scale displacements of the glass. The gap was measured interferometrically and adjusted to ~ 500 nm. In between experiments the cell could be disassembled and both pieces of glass thoroughly cleaned. The patterned piece of glass that formed the top of the cell was used for hundreds of experiments with no detectable change in its performance.

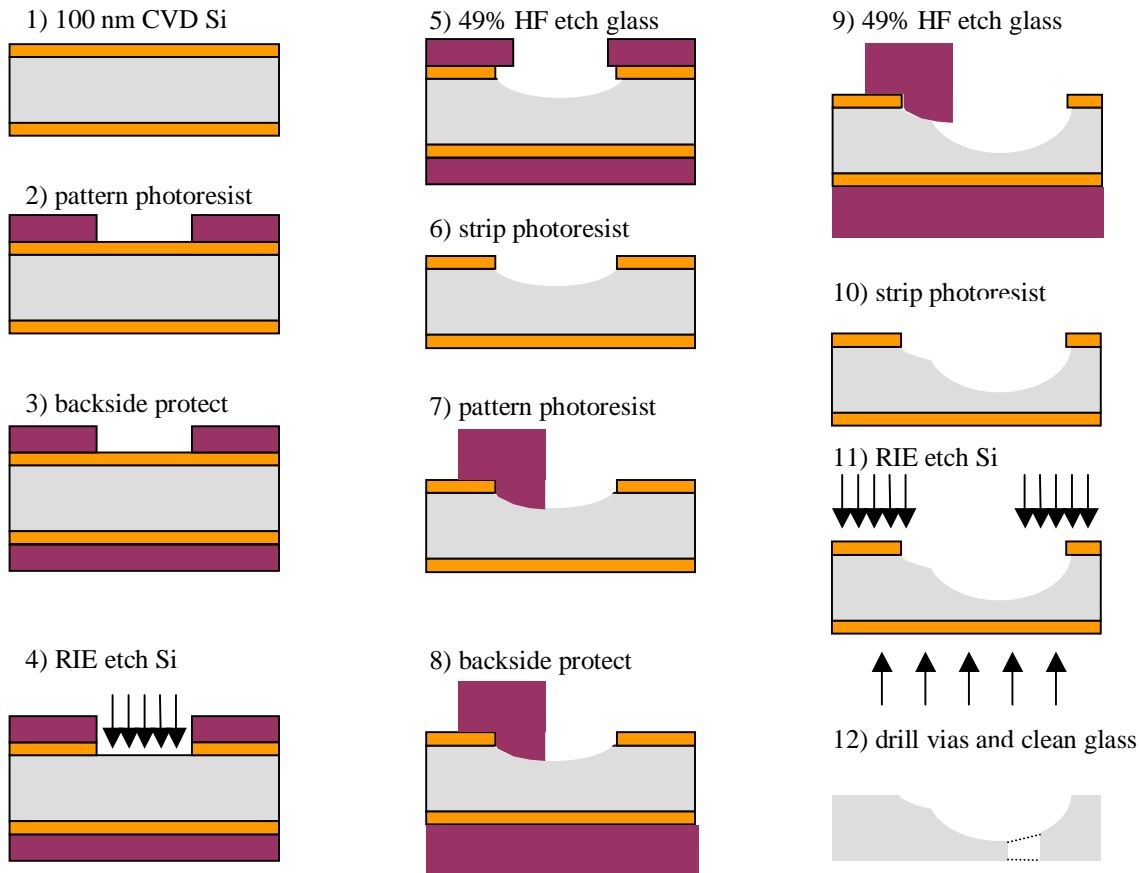


Figure 2 Process for fabricating glass microfluidic chips for the ABEL trap. The glass is patterned with two stages of photolithography and HF etching so that the channels near the trapping region are $\sim 24 \mu\text{m}$ deep, while the channels far from the trapping region are $\sim 80 \mu\text{m}$ deep. The small channel depth near the trapping region keeps adjacent channels from merging, while the greater depth further away decreases the electrical and viscous resistances of the channels.

Simulation of the electric field profile

To calculate the mobility of trapped objects it was necessary to know the conversion between voltage applied to the trap and electric field experienced by the trapped particle. A 2-dimensional finite-element simulation of the electric field was performed in Matlab. Due to their great depth (and hence high conductivity) relative to the trapping region, the channels leading to the trapping region were assumed to form equipotential surfaces. A micrograph of the trapping region was digitized, rendered in binary, and then used to set boundary conditions for the simulation (Fig. 3).

The simulations show that in the center of the trapping region the electric field is quite uniform. The field-of-view of the microscope is typically $10 \mu\text{m} \times 10 \mu\text{m}$, over which the electric field strength varies by only 0.6%. In the center of the trap, the field strength is roughly $6 \text{ (mV}/\mu\text{m})/\text{V}$. Thermal fluctuations will drive an object with a charge of $1 e$ “uphill” in the trap to a characteristic potential of $kT/e \sim 25 \text{ mV}$. To confine such a particle to a region $1 \mu\text{m}$ on a side, the field must be $\sim 25 \text{ mV}/\mu\text{m}$, which corresponds to an applied voltage of only slightly greater than 4 V . Thus, unlike traditional capillary electrophoresis systems, the ABEL trap may be operated from a low-voltage power supply.

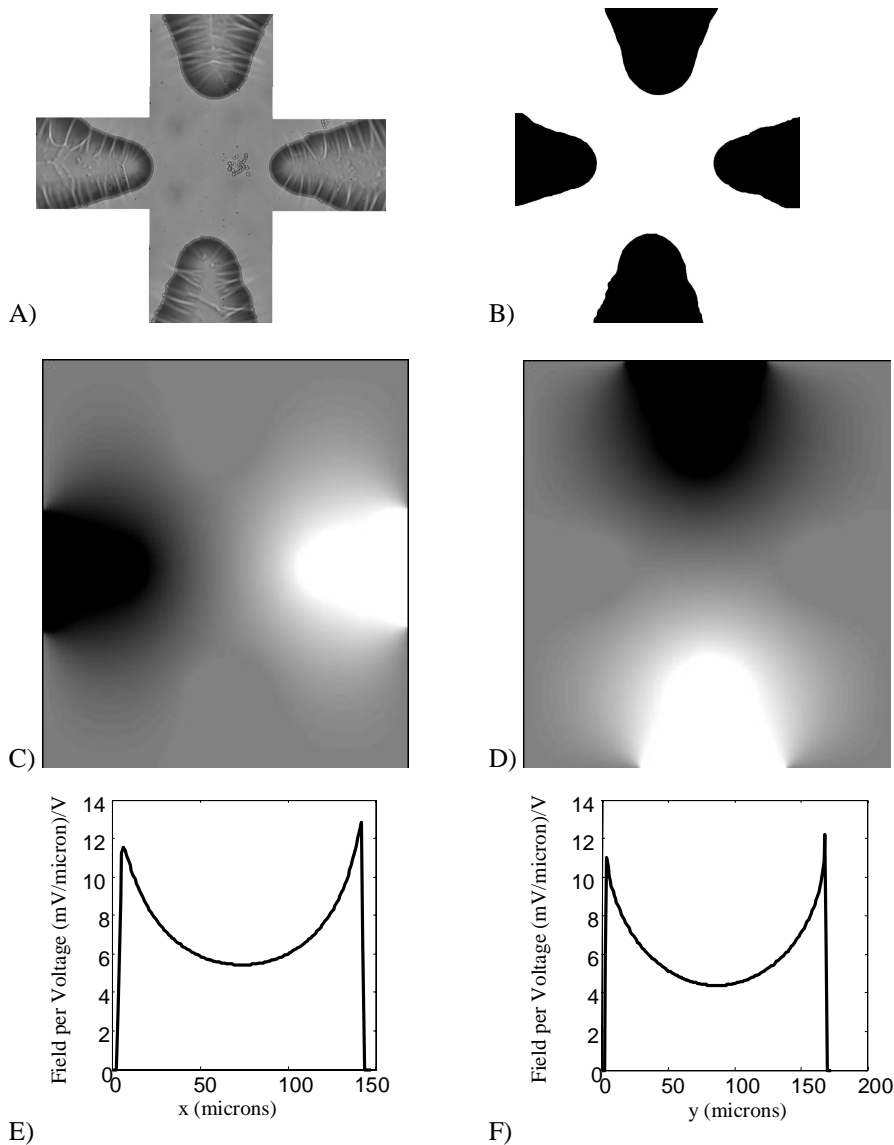


Figure 3 Numerical simulation of the electric field in the trapping region. A) composite micrograph of trapping region; B) binary version of image; C, D) potential profiles for vertical and horizontal potentials, respectively; E, F) vertical and horizontal electric field profiles through the center of the trap.

Adjusting the depth of the trapping region

It is advantageous to be able to control the depth of the trapping region. Typically one wants the depth to be small enough to confine the object under study to the focal plane of the microscope, but large enough so that the walls of the trap do not interfere with the process being studied. In some cases, such as in studies of long DNA molecules, one may wish to study the effects of confinement on the molecular conformation and dynamics.

The microfluidic cell and holder presented here give the experimenter control over the depth of the trapping region. As-assembled, the trapping region has a depth of $\sim 10 \mu\text{m}$ —too large to allow trapping. Pressing down on the

patterned slide causes the slide to bow downwards, narrowing the gap. To provide greater control over the gap, we do not push directly on the glass, but instead push on a piece of PDMS on top of the glass. Due to its high compliance, the PDMS translates a relatively large displacement at its top surface into a small force applied to the glass. In this way we are able to achieve sub-100 nm control over the thickness of the gap. Here we present a mechanical analysis of this system.

We model the cell as a simply-supported elastic plate of thickness h_g (the patterned piece of glass), with a thin rubbery sheet on top of thickness h_s (the PDMS). The set-screw pushing on the PDMS has a roughly hemispherical end-cap with radius r_b (Fig. 4). The bottom piece of glass (the coverslip), does not play a role in this analysis.

The constitutive relation of a sphere pressing on a fully supported thin elastic sheet is given by:⁸

$$\zeta_s = \left(\frac{9f}{16E_s} \right)^{2/3} r_b^{-1/3} (1 - \exp(-Ah_s / r_c)) \quad [1]$$

where ζ_s is displacement of the top of the sheet, f is the force on the sphere, E_s is the Young's modulus of the sheet, and r_c is the radius of the contact area between the sphere and the sheet, given by $r_c = r_b^{1/2} \zeta_s^{1/2}$. To achieve an analytically tractable formula, we make the approximation $r_c \approx r_b^{1/2} \zeta_\infty^{1/2}$, where ζ_∞ is the displacement that would have occurred had the sheet been infinitely thick. The exponential term is a correction for the finite thickness of the sheet, with the dimensionless factor $A = 0.4$.

Meanwhile, the constitutive relation for a simply supported elastic plate with a force applied to its center is:⁹

$$\zeta_p = \frac{f}{16\pi d} \left[\frac{3 + \sigma}{1 + \sigma} (R^2 - r^2) - 2r^2 \log \frac{R}{r} \right] \quad [2]$$

where ζ_p is the displacement, σ is Poisson's ratio, R is the radius of the support, r is the radius at which the displacement is measured, and the bending stiffness, d , is defined:

$$d = E_g h_g^3 / 12(1 - \sigma^2) \quad [3]$$

where E_g is the Young's modulus of the glass. Combining Eqs. 1- 3, one can plot the differential demagnification of the device, i.e. the ratio of the incremental displacement of the glass to an incremental displacement in the setscrew pushing on the PDMS. The result of this calculation is plotted in Fig. 4, as a function of the displacement of the setscrew. Under typical operating conditions, the demagnification is between 0.05 and 0.1. Thus the displacement of the setscrew is demagnified by a factor of 10 – 20. The setscrew has a pitch of 80 threads/inch (~315 μ m), and we can control its rotation to an accuracy of $\sim 1^\circ$. With the demagnification provided by the PDMS, this translates to a vertical displacement of the glass of 50 – 100 nm.

Conclusions

We have built and simulated an all-glass microfluidic cell for use in the ABEL trap. We expect that with this cell we will be able to trap and observe individual biomolecules for long times.

Acknowledgments AEC gratefully acknowledges the support of a Hertz Fellowship. This work was supported in part by the U. S. Department of Energy Grant No. DE FG02-04ER63777, and National Institutes of Health Grant No. 1R21-GM065331. Work was performed in part at the Stanford Nanofabrication Facility of NNIN supported by National Science Foundation under Grant ECS-9731293.

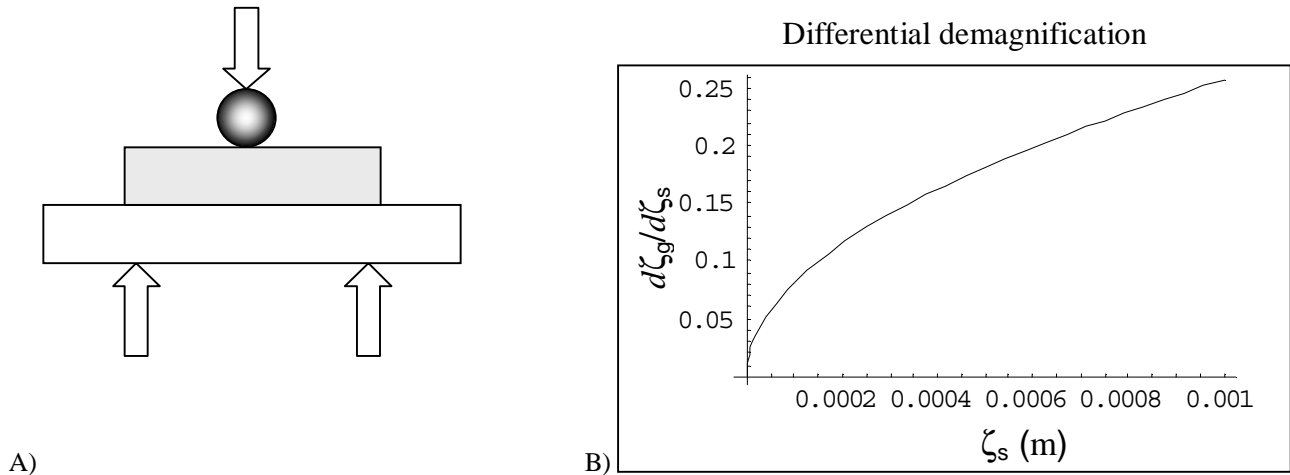


Figure 4 Mechanical analysis of the depth-control in the ABEL trap. A) A spherical indenter presses on a thin elastic sheet of PDMS, which presses on a simply supported glass plate. B) Differential demagnification. The parameters used for this plot were: for the PDMS $E_s = 0.75$ Mpa, $r_b = 1$ mm, $h_s = 3.8$ mm; for the glass $\sigma = 0.2$, $E_g = 6.4$ Gpa, $R = 2.1$ cm, and $h_g = 0.69$ mm.

¹ A. E. Cohen, W. E. Moerner, "The Anti-Brownian Electrophoretic trap (ABEL trap): fabrication and software," *Proc. SPIE* **5699**, 293 (2005).

² A. E. Cohen, "Control of nanoparticles with arbitrary two-dimensional force fields," *Phys. Rev. Lett.* **94**, 118102 (2005).

³ A. E. Cohen, W. E. Moerner, "Method for Trapping and Manipulating Nanoscale Objects in Solution," *Appl. Phys. Lett.* **86**, 093109, (2005).

⁴ H. Makamba *et al.* "Surface modification of poly(dimethylsiloxane) microchannels," *Electrophoresis* **24**, 3607 (2003)

⁵ S. Hu *et al.* "Tailoring the surface properties of poly(dimethylsiloxane) microfluidic devices," *Langmuir* **20**, 5569 (2004).

⁶ D. Belder and M. Ludwig, "Surface modification in microchip electrophoresis," *Electrophoresis* **24**, 3595 (2003).

⁷ J. Gaudioso and H. G. Craighead, "Characterizing electroosmotic flow in microfluidic devices," *J. Chromatography A* **971**, 249 (2002).

⁸ N. E. Waters, "The indentation of thin rubber sheets by spherical indentors," *Brit. J. Appl. Phys.* **16**, 557 (1965).

⁹ L. D. Landau and E. M. Lifshitz, (transl. J. B. Sykes and W. H. Reid), *Theory of Elasticity* Ch. 2, problem 4, Butterworth Heinemann, Boston, 1986.